

RESEARCH PAPER



USP7-mediated deubiquitination differentially regulates CSB but not UVSSA upon UV radiation-induced DNA damage

Qianzheng Zhu^a, Nan Ding^{a*}, Shengcai Wei^a, Ping Li^a, Gulzar Wani^a, Jinshan He^a, and Altaf A. Wani^{a,b,c}

^aDepartment of Radiology, The Ohio State University College of Medicine, Columbus, OH, USA; ^bDepartment of Molecular and Cellular Biochemistry, The Ohio State University College of Medicine, Columbus, OH, USA; ^cJames Cancer Hospital and Solove Research Institute, The Ohio State University, Columbus, OH, USA

ABSTRACT

Cockayne syndrome group B (CSB) protein participates in transcription-coupled nucleotide excision repair. The stability of CSB is known to be regulated by ubiquitin-specific protease 7 (USP7). Yet, whether USP7 acts as a deubiquitinating enzyme for CSB is not clear. Here, we demonstrate that USP7 deubiquitinates CSB to maintain its levels after ultraviolet (UV)-induced DNA damage. While both CSB and UV-stimulated scaffold protein A (UVSSA) exhibit a biphasic decrease and recovery upon UV irradiation, only CSB recovery depends on USP7, which physically interacts with and deubiquitinates CSB. Meanwhile, CSB overexpression stabilizes UVSSA, but decrease UVSSA's presence in nuclease-releasable/soluble chromatin, and increase the presence of ubiquitinated UVSSA in insoluble chromatin alongside CSB-ubiquitin conjugates. Remarkably, CSB overexpression also decreases CSB association with USP7 and UVSSA in soluble chromatin. UVSSA exists in several ubiquitinated forms, of which mono-ubiquitinated form and other ubiquitinated UVSSA forms are detectable upon 6xHistidine tag-based purification. The ubiquitinated UVSSA forms, however, are not cleavable by USP7 *in vitro*. Furthermore, USP7 disruption does not affect RNA synthesis but decreases the recovery of RNA synthesis following UV exposure. These results reveal a role of USP7 as a CSB deubiquitinating enzyme for fine-tuning the process of TC-NER in human cells.

ARTICLE HISTORY

Received 18 September 2019
Revised 16 October 2019
Accepted 5 November 2019

KEYWORDS

Ubiquitin-specific protease 7 (USP7); nucleotide excision repair (NER); transcription-coupled nucleotide excision repair (TC-NER); Cockayne syndrome group B (CSB); ultraviolet radiation (UVR)-stimulated scaffold protein A (UVSSA); valosin-containing protein (VCP)/p97

Introduction

Nucleotide excision repair (NER) eliminates a broad variety of helix-distorting DNA lesions, including ultraviolet radiation (UVR)-induced cyclobutane pyrimidine dimers (CPDs) and 6–4 photoproducts (6-4PPs) [1–3]. The mammalian NER consists of two distinct sub-pathways: the global genomic NER (GG-NER), which operates throughout the genome, and the transcription-coupled NER (TC-NER), which eliminates DNA damage from transcribed DNA strands of transcriptionally active genes [4,5]. Impaired NER activity is associated with several rare autosomal recessive genetic disorders, e.g. Xeroderma pigmentosum (XP) [6] and Cockayne syndrome (CS) [7–9].


CSA and CSB, two CS gene-encoded proteins, function in TC-NER, which sense DNA lesions by stalling of elongating RNA polymerase II (RNAPII) [10,11]. The lesion-arrested RNAPII, together with

CSB, initiates the process of TC-NER [12–15]. In particular, the RNAPII-CSB complex recruits CSA, transcription factor II H (TFIIH), and other core NER factors, as well as non-NER factors to the lesion sites [16]. The transcription elongation process subsequently funnels into the assembling of common pre-precision complex of NER. Successful TC-NER removes DNA lesions from transcribed strand, allowing the recovery of RNA synthesis (RRS), which indirectly indicates successful TC-NER.

CSB protein undergoes ubiquitin (Ub)-mediated proteolysis during TC-NER of photolesions [17,18]. Valosin-containing protein (VCP)/p97 segregase extracts ubiquitin-CSB conjugates from chromatin and presented them to proteasome for proteolysis [18]. Recent identification and study of two new TC-NER factors have further revealed that UV-stimulated scaffold protein A (UVSSA) and Ub-specific protease 7 (USP7) jointly control the cellular level of CSB after

CONTACT Altaf A. Wani ✉ wani.2@osu.edu; Qianzheng Zhu ✉ zhu.49@osu.edu

*Present address: Department of Space Radiobiology, Institute of Modern Physics, Chinese Academy of Sciences, Chengguan District, Lanzhou, China 730000.

 Supplementary data for this article can be accessed [here](#).

© 2019 Informa UK Limited, trading as Taylor & Francis Group

UVR exposure, thereby regulating TC-NER [19–21]. For example, both UVSSA and USP7 are required to maintain the CSB level after cellular UVR exposure. It is known that UVSSA is recruited to DNA damage sites in CSA-dependent manner and that UVSSA interacts with RNAPII, CSB, and USP7 [19,20]. Yet, it is unclear how cellular CSB level or its Ub-mediated degradation is regulated by USP7 [9]. Whether USP7 acts as a deubiquitinating enzyme (DUB) for CSB remains to be established.

USP7 is a known DUB for tumor suppressor p53 and Mdm2 [22,23]. USP7 rescues p53 and Mdm2 proteins from proteolysis by removing Ub moieties from the Ub-conjugated proteins. USP7 disruption in HCT116 cells leads to the stabilization of p53, slow cell growth and cellular morphological changes [24]. Our previous work identified USP7 as a DUB for XPC [25], a damage recognition factor of GG-NER, and for RNF168 [26], an E3 ligase of Ub signaling cascade. In the present study, we investigated the nature of biphasic decrease and recovery of CSB observed upon UVR-induced DNA damage in human cells. We have revealed that USP7 also acts as a specific DUB for CSB.

Results

USP7 is essential for late-phase CSB recovery following UVR-induced DNA damage

We first investigated the effect of UVR on CSB levels in cells with well-defined USP7 status, designated HCT116 and HCT116-USP7^{-/-} [24,25]. In our experiments, CSB antibodies B10 and A301-345 were verified by their recognition of FLAG- and Myc-tagged CSB protein in cDNA-transfected HeLa cells (Figure S1), while CSB antibody E-18 was verified by its recognition of Dox-induced CSB protein in cDNA-corrected CSB-deficient CS1AN cells (Figure 1(b)). We noticed that these CSB antibodies react with specific CSB band and uncharacterized protein bands of smaller sizes in both HCT116 and HeLa cells (Figure 1(a,b) and Figure S1). Importantly, the CSB levels of the specific band in USP7-proficient parental HCT116 cells exhibited a clear biphasic response, with an initial decrease and then an increase following UVR exposure. The maximum decline was seen at ~4 h and a steady recovery was seen in 8-h to 24-h period (Figure 1(a–c)), in

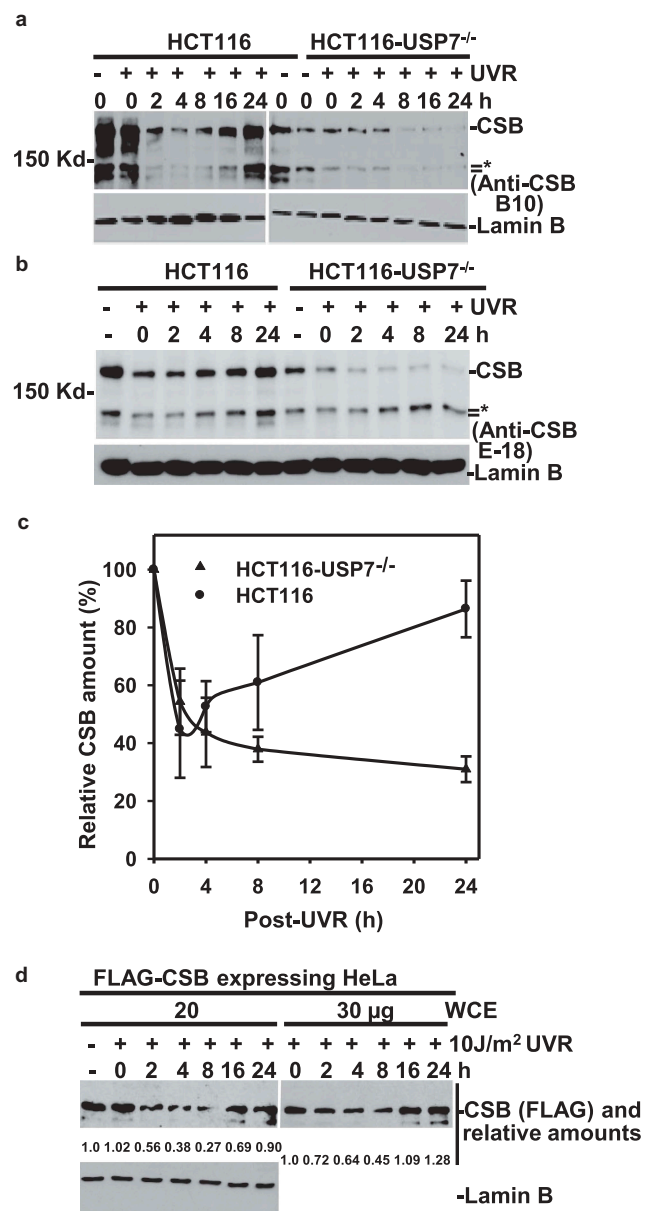


Figure 1. USP7 deficiency prevents the recovery of CSB protein following UVR-induced DNA damage. (a) HCT116 and HCT116-USP7^{-/-} cells were irradiated at 10 J/m² and CSB levels post-UVR in whole-cell extracts (WCE) were determined using CSB antibody B10. Lamin B blot was used as a loading control. (b) HCT116 and HCT116-USP7^{-/-} cells were irradiated at 10 J/m² and maintained as in (A). The WCE were Western blotting analyzed using CSB antibody E-18. (c) CSB levels detected using CSB antibody E-18 in HCT116-USP7^{+/+} or HCT116-USP7^{-/-} from three independent experiments were quantitated by ImageJ software. The average relative CSB amounts with SE (standard error, SE) were presented in comparison with unirradiated controls. (d) HeLa-derived #57 cells (HeLa#57), expressing FLAG- and Myc-tagged CSB protein, were exposed to 10 J/m² UVR and kept for indicated post-UVR periods. The FLAG-tagged CSB levels in WCE were detected by Western blotting using anti-FLAG antibody. The relative amount of FLAG-tagged CSB in representative CSB blots was calculated by comparison with unirradiated control upon quantitation by ImageJ software. Asterisks (*) mark nonspecific bands in anti-CSB blots.

which, RNA synthesis got eventual full recovery after the completion of TC-NER (Figure 9). Notably, the CSB levels in HCT116-USP7^{-/-}, lower than that in parental HCT116, also exhibited a UVR-induced initial decrease but failed to recover at later post-UV period. UV irradiation at 10 J/m² dose significantly decreased CSB in USP7-deficient cells after 8 h. The biphasic response of cellular CSB also occurs in HeLa-derived cells expressing FLAG-tagged CSB (Figure 1(d)). Whereas, the maximum decline of FLAG-tagged CSB in HeLa cells was seen at 8 h following 10 J/m² UVR under two different both loading schemes. Taken together, these results revealed that UVR-induced DNA damage triggers a biphasic response of cellular CSB.

We have previously demonstrated that UVR induces a VCP/p97-regulated and Ub-mediated CSB proteolysis in human cells [18]. As the UV irradiation causes greater CSB loss in HCT116-USP7^{-/-} cell at earlier (~4–8 h) periods and without observable recovery at later (8–24 h) periods, we reasoned that proteolysis might affect CSB recovery. We, therefore, examined endogenous CSB ubiquitination through the analysis of CSB-Ub conjugates. Under optimized conditions, three <250 Kd modified forms of CSB were detected in both HCT116 and HCT116-USP7^{-/-} cells (Figure 2(a)). These <250 Kd modified forms of CSB were previously reported to be dependent on CRL4^{CSA} E3 ligase [17,27]. The lower levels of CSB and its modified forms notwithstanding, the pattern of modified CSB forms in USP7^{-/-} HCT116 cells remained the same as that in USP7^{+/+} HCT116 cells. Upon enrichment through anti-CSB immunoprecipitation, the >250 Kd modified CSB forms were also detected, especially in cells irradiated at 20 J/m² dose (Figure 2(b)). It was previously reported that CSB is modified by SUMO2/3 at molecular weights >250 Kd [28]. We, therefore, attempted to detect CSB SUMOylation in anti-CSB immunoprecipitates. The presence of >250 Kd SUMO (2/3)-modified forms of CSB was seen at relatively higher UVR doses, i.e., 50 and 100 J/m². The absence of CSB SUMOylation signal at 20 J/m² may be due to relatively low levels of SUMOylated CSB species. It is possible that there are >250 Kd ubiquitin-SUMO modified CSB forms.

To verify CSB ubiquitination forms >250 Kd, we next performed GST pull-down assay with a GST fusion protein containing proteasomal Ub receptor S5a, which binds poly-ubiquitin chains (Figure 2(c)) [29]. As expected, GST-S5a retained Ub-modified XPC forms mainly in <150 Kd range. By contrast, GST-S5a distinctly retained >250 Kd modified CSB forms, indicating that this portion of modified CSB is polyubiquitinated and has high affinity to proteasomal S5a. Unsurprisingly, the S5a retained USP7, due presumably to its five Ub-like (UBL) domains. Whereas, S5a was not able to retain TFIIH components XPD and XPB, which are not ubiquitinated after UV exposure. The polyubiquitinated CSB species were further confirmed using 6xHistidine-tagged Ub and Ni-NTA-based enrichment of Ub conjugates of FLAG- and Myc-tagged CSB (Figure 7(a)). To conclude, CSB undergoes UVR-induced modifications with a wide range of Ub moieties.

USP7 deficiency reduces steady-state level of UVSSA but USP7 is not essential for late-phase UVSSA recovery after UVR-induced DNA damage

Since USP7 was reported to stabilize UVSSA through protein-protein interaction [30], we also examined the fate of UVSSA in response to UVR. In parental HCT116 cells, the UVSSA levels exhibited a slight but identifiable biphasic response in parental HCT116 cells (Figure 3(a)). The UVSSA protein appeared to be double-banded in HCT116-USP7^{-/-} cells and the level was slightly higher than that in parental HCT116 cells. Upon UVR exposure, UVSSA levels showed a clear biphasic response, with a sharp decrease from 2 to 8 h and a strong recovery from 16 to 24 h in HCT116-USP7^{-/-} cells (Figure 3(b)). These results suggest that the USP7 function is not required for UVSSA level recovery.

Next, we determined whether the UVR-induced UVSSA decrease in HCT116 was a result of Ub-mediated proteolysis. An increased UV dose (50 J/m²) was used to induce discernable elimination of both UVSSA and CSB and to examine the effect of proteasome inhibitor MG132 and VCP/p97 inhibitor DBeQ at 8 h (Figure 3(c)). The treatments, with either MG132 or DBeQ, partly rescued the loss of UVSSA. In parallel, both inhibitors also reduced the UVR-induced CSB degradation (Figure 3(c)). Additionally, the UVR-induced CSB degradation

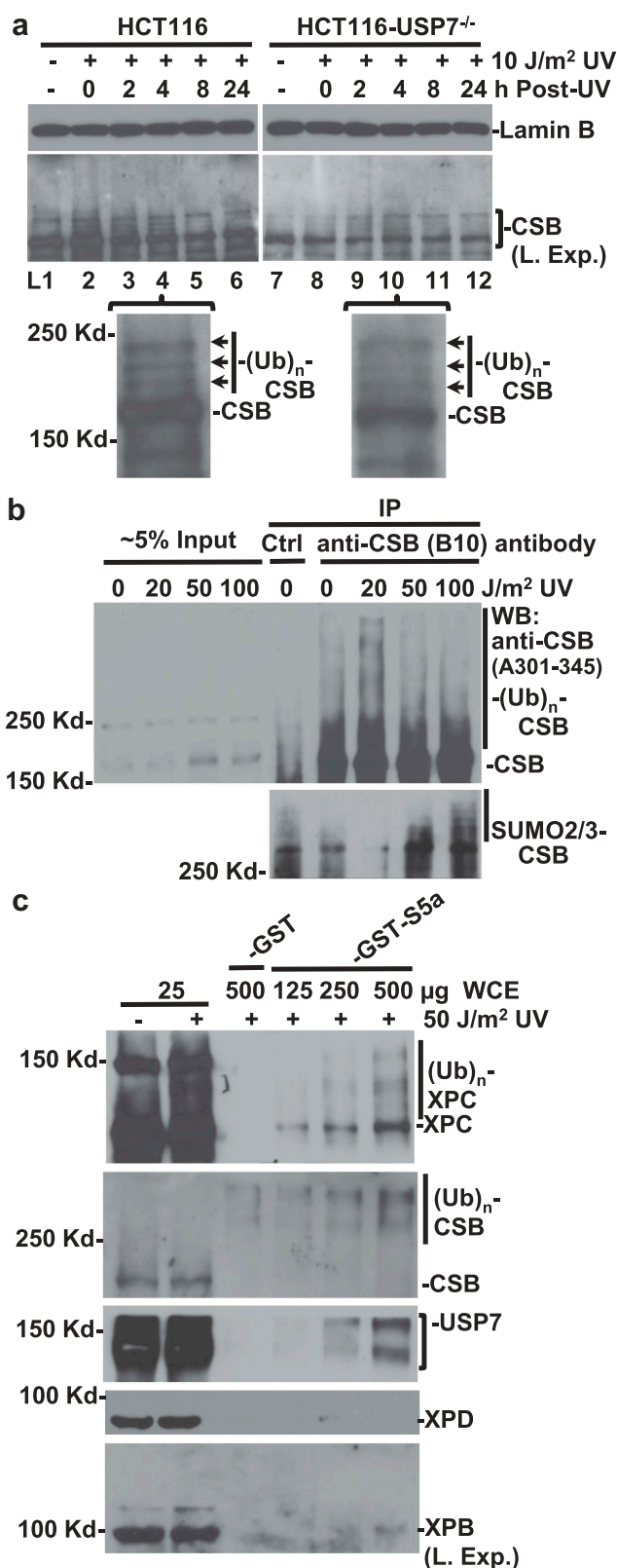


Figure 2. UVR-induced DNA damage triggers CSB ubiquitination. (a) HCT116 and HCT116-USP7^{-/-} cells are irradiated as in Figure 1. The modified CSB forms were detected in WCE by Western blotting through a comparatively longer time exposure (L. Exp.) of chemiluminescent detection. Indicated lanes from two blots were enlarged for clearer band visualization. (b) Control and UV-irradiated HCT116 cell lysates in RIPA buffer were subjected to immunoprecipitation by mouse CSB antibody B10 and the immunoprecipitates were Western blotting analyzed for modified CSB forms with rabbit CSB antibody and SUMO-2/3 antibody. (c) GST pull-down assays were performed with WCE from UV-irradiated HCT116 cells using GST and GST-S5a immobilized glutathione beads. Proteins retained by GST-S5a were detected with anti-XPC, CSB, USP7, XPB or XPD specific antibodies.

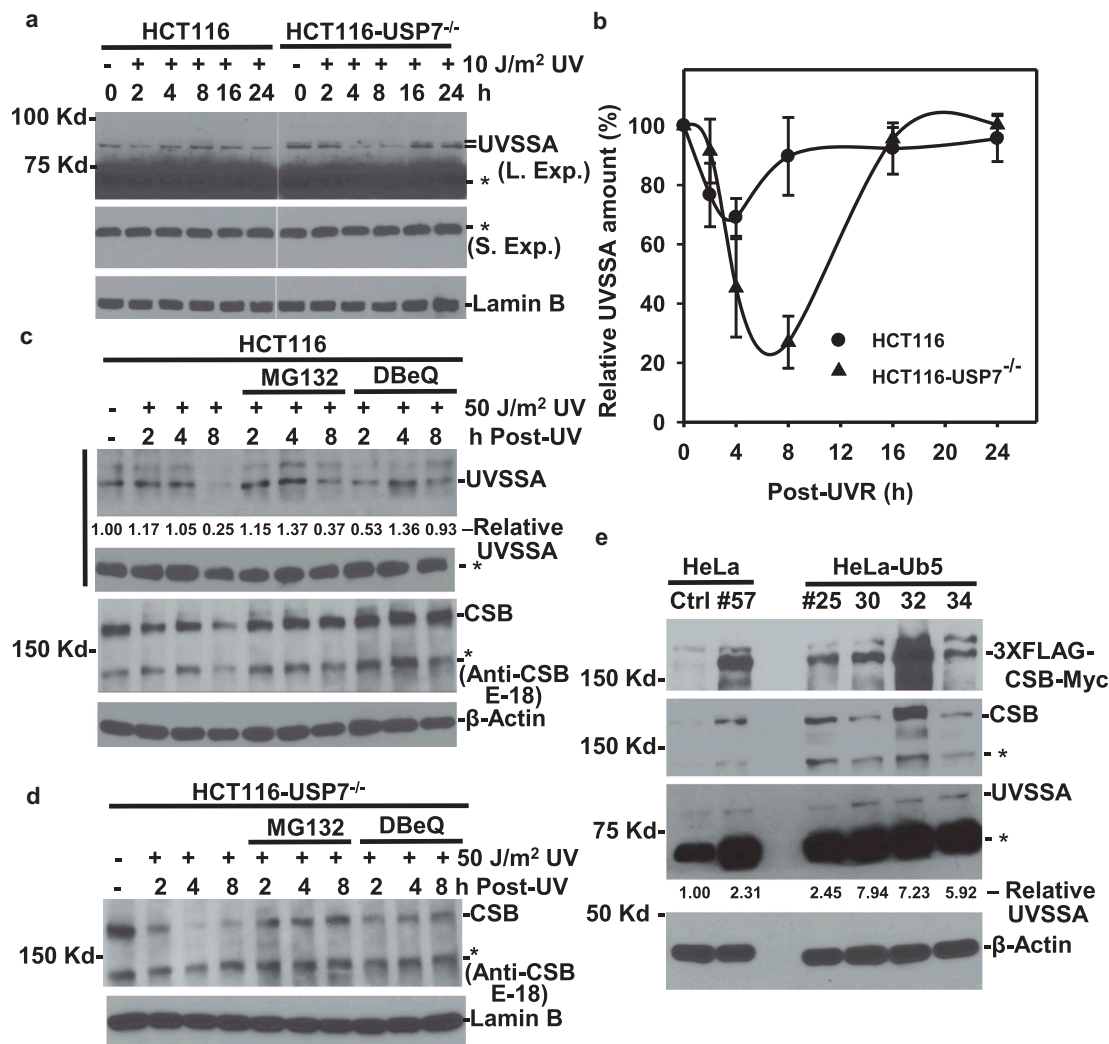


Figure 3. Effect of UV irradiation, USP7 disruption and CSB overexpression on UVSSA. (a) HCT116 and HCT116-USP7^{-/-} cells are irradiated as in Figure 1. UVSSA levels were detected by Western blotting using UVSSA specific antibody. "S. Exp." represents the short time film exposure. (b) The blots from more than three independent experiments were quantitated by ImageJ software. The relative UVSSA amounts were calculated and normalized in comparative to unirradiated controls and used with SE for the plots. (c) HCT116 cells were UV-irradiated and then treated with proteasome inhibitor MG132 or VCP/p97 inhibitor DBeQ for indicated periods. The WCE were Western blotting analyzed for UVSSA and CSB, using different specific antibodies. β-Actin blots served as an equal loading control. (d) HCT116-USP7^{-/-} cells were treated similarly to that in (C) and the WCE were Western blotting analyzed for CSB. (e) FLAG- and Myc-tagged CSB proteins were stably expressed in HeLa-derived #57 cells or HeLa-Ub5-derived #25, 30, 32, 34 cells, which also harbor a 6xHistidine-tagged Ub. The stable cell lines were examined for FLAG-tagged CSB, CSB, UVSSA, and β-Actin. "L. Exp." represents the longer time film exposure. The relative UVSSA amount in each cell lines was calculated in comparison with HeLa control, based on quantitation of the specific bands by ImageJ software. Asterisks (*) mark nonspecific bands in all anti-CSB and UVSSA blots.

via VCP/p97 and proteasome was validated in UVR-treated HCT116-USP7^{-/-} cells, where CSB underwent more noticeable loss (Figure 3(d)). Thus, UVSSA undergoes a partial Ub-mediated and VCP/p97-regulated proteolysis in the early phase of cellular UV response. However, UVSSA level recovery in the late phase, unlike CSB, does not require USP7.

We established several HeLa-derived cell lines with enforced FLAG-tagged CSB expression at moderate to relatively high levels (Figure 3(e)). An examination of

UVSSA in these cell extracts showed that UVSSA levels were elevated in coincidence with CSB expression in all FLAG-tagged CSB-expressing cell lines (Figure 3(e)). Thus, CSB appears to stabilize UVSSA in the absence of DNA damage.

USP7 physically interacts with CSB and VCP/p97

Next, we examined the physical interaction between USP7 and CSB by GST pull-down assay using bacterially expressed GST-USP7 fusions, as we previously

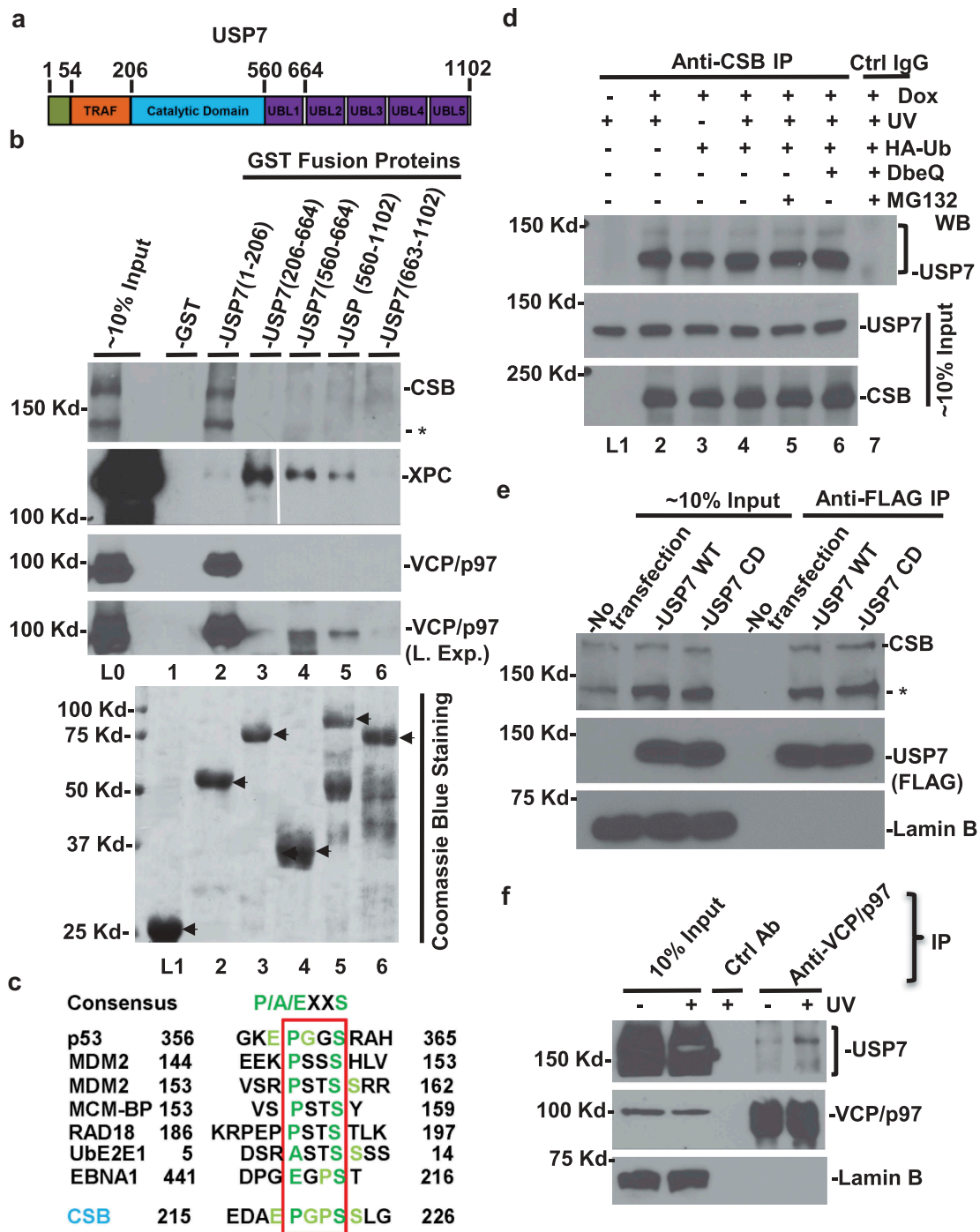


Figure 4. Interactions of CSB, USP7 and VCP/p97. (a) Diagrammatic representation of USP7 domains. (b) GST pull-down assays were performed with RIPA extracts from UV-irradiated HCT116 cells using glutathione bead-immobilized GST fusion proteins containing the indicated USP7 segments. The retained proteins were examined for CSB, XPC and VCP/p97 with different specific antibodies. "L. Exp." was to show weaker VCP/p97 bands in GST pull-down assays. Lower panel showed a Coomassie blue staining of immobilized GST fusion. (c) Alignment of TRAF recognition motif found in 215–226 amino acid of CSB protein with the motifs in other USP7 substrates. The green letters represent consensus amino acids in the motif (P/A/EXXS); letter X represents any amino acid; light green letters represent common but less restricted amino acids. (d) The cellular CSB-USP7 interactions were detected using the corrected CS1AN cells with doxycycline (Dox)-inducible CSB expression. The corrected CS1AN cells, transiently expressing HA-Ub, were induced for CSB expression with 1 μ g/ml Dox for 24 h. The transfected cells were then UV irradiated, treated with MG132 or DBeQ or vehicle DMSO and maintained for 6 h. The cell lysates were prepared for immunoprecipitation with CSB or control antibody, followed by Western blotting analysis for the presence of CSB and USP7 in immunoprecipitates. (e) The FLAG-tagged WT and catalytic dead (CD) USP7 mutant were transiently expressed in HCT116 cells. The immunoprecipitations were performed using anti-FLAG gels and the presence of CSB in immunoprecipitates was examined by Western blotting. The asterisk (*) marks the nonspecific band recognized by CSB antibody. (f) Immunoprecipitation experiments were performed using VCP/p97 specific antibody and HCT116 cell extracts made from control or UV treated cells in RIPA buffer. Lamin B blots in Figure 4(e, f) served as equal loading controls.

reported [25]. The GST fusion protein containing the USP7 N-terminal, spanning 1 to 206 amino acid (AA) (Figure 4(a,b)), retained CSB and VCP/p97 (Figure 4(b)). Longer exposures showed that USP7 UBL1 also weakly retained VCP/p97. By contrast, USP7 UBL1 (560–644 AA) showed a clear retention of XPC (Figure 4(b)) [25]. It is noteworthy that the USP7 N-terminal contains a tumor necrosis factor receptor-associated factor (TRAF) domain (Figure 4(a)), which serves as a substrate-interacting domain for many USP7 substrates [31,32]. Upon amino acid alignment, a TRAF recognition motif with P/A/EXXS consensus was found in 215–226 AA of CSB protein (Figure 4(c)). This USP7 TRAF recognition motif is different from the USP7 UBL1 recognition motif (also called KXXXXK motif), which exists in XPC within 328 to 440 AA [33], suggesting that USP7 may recognize CSB and XPC using a different binding mechanism.

The cellular USP7-CSB interaction was further examined by co-immunoprecipitation. As shown in Figure 4(d), upon Dox-induced cellular CSB expression, USP7 was seen in anti-CSB immunoprecipitates regardless of UVR-induced DNA damage, Ub-tagging, proteasome or VCP/p97 inhibition. These results were consistent with reported USP7-CSB interaction occurring even without UVR [19,20]. We also conducted a reciprocal immunoprecipitation of FLAG-tagged wild type (WT) USP7 and catalytic dead (CD) mutant USP7 in a transient expression experiment (Figure 4(e)). The USP7 CD contains a cysteine to serine substitution at amino acid (AA) 223, which specifically inactivates the deubiquitinating activity of USP7. Yet, both WT and CD USP7 were able to associate with CSB. Similarly, in a confirmatory anti-VCP/p97 immunoprecipitation, USP7 was shown to associate with VCP/p97 in cells (Figure 4(f)) and, the UVR clearly enhanced the USP7-VCP/p97 association. To conclude, USP7 physically interacts with CSB and VCP/p97.

USP7 deubiquitinates CSB

To examine the cellular deubiquitinating activity of USP7 toward CSB, we carried out transient transfections to express various tagged proteins and assessed the modified CSB forms through immunoprecipitation followed by Western blotting analysis. Direct evaluation of

input from transfected cells revealed a clear accumulation of HA-tagged Ub conjugates when proteasome was inhibited (Figure 5(a)). The lysates from CSB and/or USP7 construct transfected cells showed cognate exogenous CSB and USP7 expression (Figure 5(a), L2-6). Recovery of CSB by anti-FLAG immunoprecipitation, followed by anti-HA immunoblotting revealed distinct CSB-Ub conjugates in MG132 treated samples (Figure 5(b), L3 and L4). More importantly, a clear reduction in CSB-Ub conjugates was seen in the company with exogenous USP7 expression. Confirmation through anti-Myc immunoprecipitation further indicated that USP7 indeed deubiquitinates CSB-Ub conjugates in cells (Figure 5(b), lower panel). In similar experiments, where both WT and CD USP7 were included, WT USP7 reduced CSB-Ub conjugates while CD USP7 did just the opposite (Figure 5(c), L3, 4 and 5). Thus, USP7 cleaves Ub moieties from CSB-Ub conjugates in cells.

To demonstrate CSB deubiquitination by USP7 *in vitro*, we utilized both soluble and insoluble chromatin fractions from UVR-treated HeLa-Ub5#32 cells for substrate preparation. These established cells stably express epitope-tagged CSB at high level and harbor 6xHistidine-tagged Ub. The CSB-Ub conjugates were loaded on anti-FLAG affinity gels to perform CSB deubiquitination. Western blotting analysis of untreated substrates showed that <250 Kd CSB-Ub conjugates existed in both chromatin fractions, while >250 Kd CSB-Ub conjugates existed primarily in insoluble chromatin fractions (Figure 5(d); also described later in Figures 6 and 7). USP7 was able to cleave CSB-Ub conjugates from both <250 Kd and >250 Kd ubiquitinated forms. Since the insoluble chromatin fractions were solubilized in SDS lysis buffer and diluted 20-fold prior to anti-FLAG gel loading, trace endogenous UVSSA would have been inactive. We concluded that USP7 alone can deubiquitinate CSB *in vitro*.

Overexpression of CSB leads to accumulation of CSB- and UVSSA-Ub conjugates in insoluble chromatin fraction

Next, we examined the distribution of CSB-Ub conjugates in soluble and insoluble chromatin

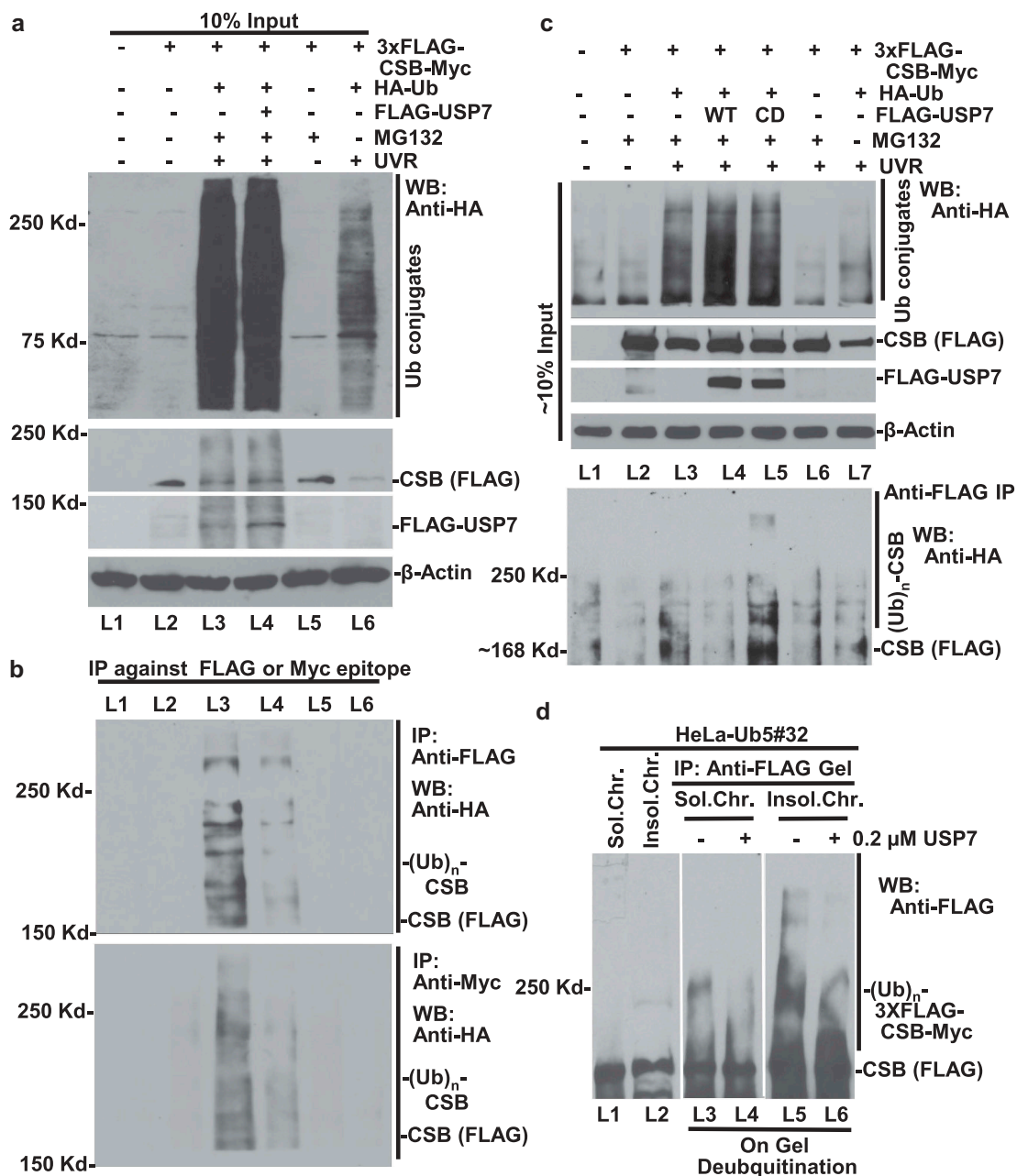


Figure 5. Deubiquitination of CSB-Ub conjugates by USP7. (a) HeLa cells were transiently transfected either alone or in the combination of the expression constructs of epitope-tagged CSB, Ub, and USP7. The total DNA amount of each transfection was kept the same by adding an empty vector. The transfected cells were UV irradiated and followed by immediate treatment with MG132 for 6 h or no treatment as controls. The cell lysates were made in RIPA buffer and Western blotting analyzed for Ub conjugates, CSB, USP7, and β -Actin, and the results were labeled as "Input". (b) The cell lysates shown in Figure 5(a) were subjected to immunoprecipitation with Anti-FLAG or Anti-Myc affinity gels, followed by detection of CSB-Ub conjugates with anti-HA antibody. (c) HeLa cells were transiently transfected and the experiments were carried out similarly to that in Figure 5(a), except that both FLAG-tagged WT USP7 and catalytic dead (CD) mutant were included in transfections. (d) Soluble and insoluble chromatin fractions were isolated from HeLa-Ub5#32 stable cells expressing FLAG-tagged-CSB. The fractions were diluted 20-fold in RIPA for protein pull-down with anti-FLAG affinity gel and the USP7 deubiquitination assays were done with gel-associated CSB forms.

fractions from cell lines expressing different levels of tagged CSB. In these cellular protein fractionation experiments, Benzonase nuclease, a highly active DNA and RNA endonuclease, was used to

digest chromatin to obtain nuclease-releasable/soluble chromatin fractions. The fractions pelleted by centrifugation after Benzonase digestion were described as insoluble chromatin fractions.

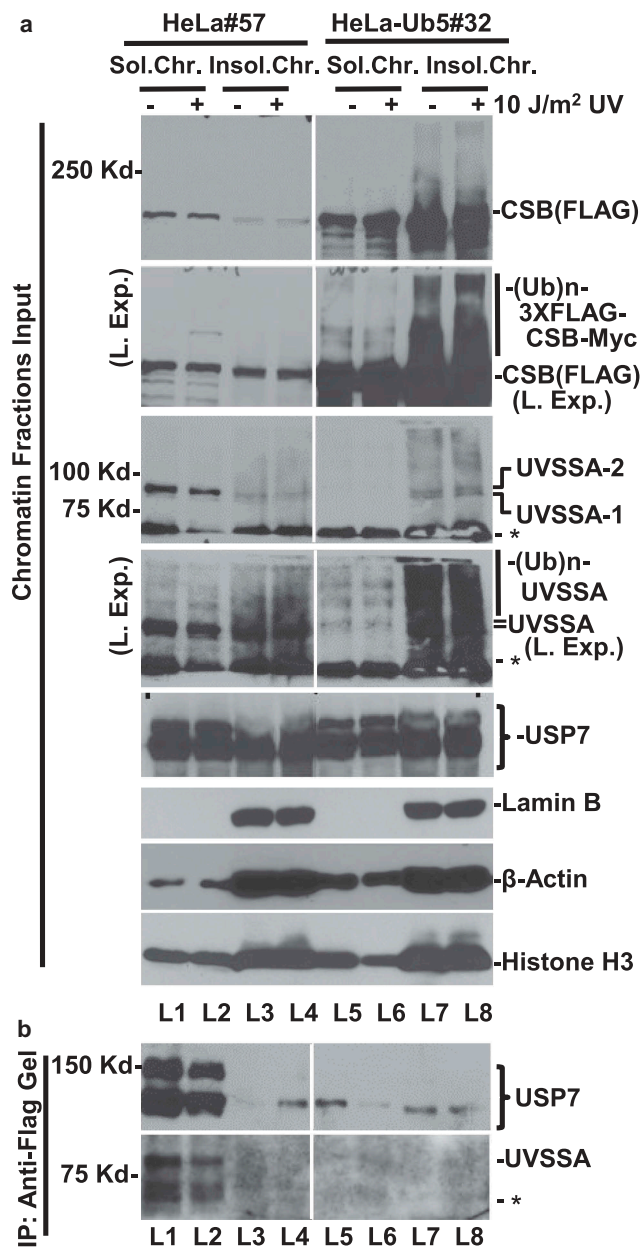


Figure 6. CSB overexpression decreases UVSSA from soluble chromatin and promotes UVSSA to insoluble chromatin fractions. (a) Soluble and insoluble chromatin fractions were isolated from CSB-expressing HeLa#57 and HeLa-Ub5#32 stable cell lines, the latter harbors a 6xHistidine-tagged Ub. Various protein fractions from each cell line were examined for the presence of CSB, UVSSA, and USP7. (b) The fractions in Figure 6(a) were used for immunoprecipitation in RIPA buffer with anti-FLAG affinity gel. For insoluble fractions, equivalent amount of fractions was diluted 20-fold in RIPA buffer then were used for the gel immunoprecipitation. The immunoprecipitates were Western blotting analyzed for the presence of USP7 and UVSSA. IP lanes L1 to L8 correspond to Input lanes L1 to L8. Asterisk (*) marks the persistent nonspecific band in anti-UVSSA blots. Blots of β-Actin, Lamin B and histone H3 served as indicators for chromatin fractions. All Western blotting analyses were done with single polyacrylamide gel, while empty lanes were digitally removed for presentation.

As expected, heterochromatin marker Lamin B only existed in insoluble chromatin fractions, while Histone H3 and β-actin existed in both fractions with extra in insoluble chromatin fractions (Figure 6(a)). Importantly, HeLa#57 cells,

expressing moderate levels of CSB transgene, showed low but detectable FLAG-tagged CSB in both fractions, while CSB-Ub conjugates were undetectable (Figure 6(a)). By contrast, in CSB highly expressed HeLa-Ub5#32 cells, CSB-Ub

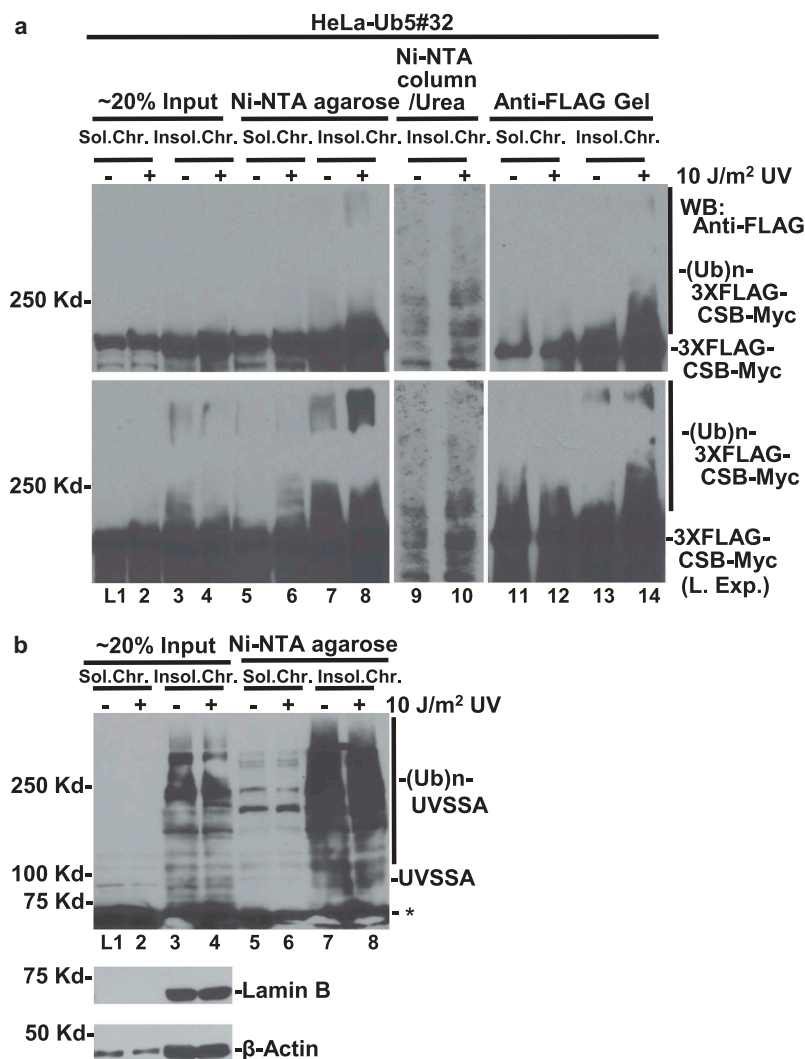


Figure 7. Detection of ubiquitinated CSB and UVSSA in chromatin fractions. (a) Soluble and insoluble chromatin fractions were isolated from CSB-expressing HeLa-Ub5#32 stable cells. The chromatin fractions were subjected to immunoprecipitation using Ni-NTA agarose or anti-FLAG (CSB) affinity gel in RIPA buffer or Ni-NTA spin column (lane 9 and 10) with urea-solubilized insoluble chromatin fractions. Proteins retained on agarose, gel or spin column were Western blotting analyzed for FLAG-tagged CSB. Longer time exposure (L. Exp.) is to show Ub conjugates of CSB with high molecular mass. (b) The retained proteins were Western blotting analyzed for UVSSA. Asterisk (*) marks nonspecific band in anti-UVSSA blot.

conjugates (verified and described later in [Figure 7 \(a\)](#)) were clearly detected in insoluble chromatin fractions.

An examination of UVSSA indicated that UVSSA in HeLa#57 soluble chromatin fraction existed in two forms, with a prominent upper band (UVSSA-2) ([Figure 6\(a\)](#)). By contrast, the two UVSSA forms appeared as faint indistinguishable smears in insoluble chromatin fractions. Despite the higher UVSSA level in HeLa-Ub5#32 than in HeLa#57 cells ([Figure 3\(e\)](#)), the UVSSA was largely restricted to insoluble chromatin fraction in HeLa-Ub5#32 cells. Moreover, the larger molecule

smear of modified UVSSA was distinctively visible in HeLa-Ub5#32 than in HeLa #57 cells, suggesting the existence of ubiquitinated UVSSA (verified and described later in [Figures 7\(b\)](#) and [Figure 8](#)) in insoluble chromatin fraction. Unlike UVSSA and CSB proteins, the known dual forms of USP7 distributed uniformly in both chromatin fractions. The presence of ubiquitinated CSB and UVSSA in insoluble chromatin fraction per se does not necessarily suggest their tight association with chromatin. Yet, these results suggest that the overexpressed CSB affects UVSSA ubiquitination and its presence in insoluble chromatin fraction.

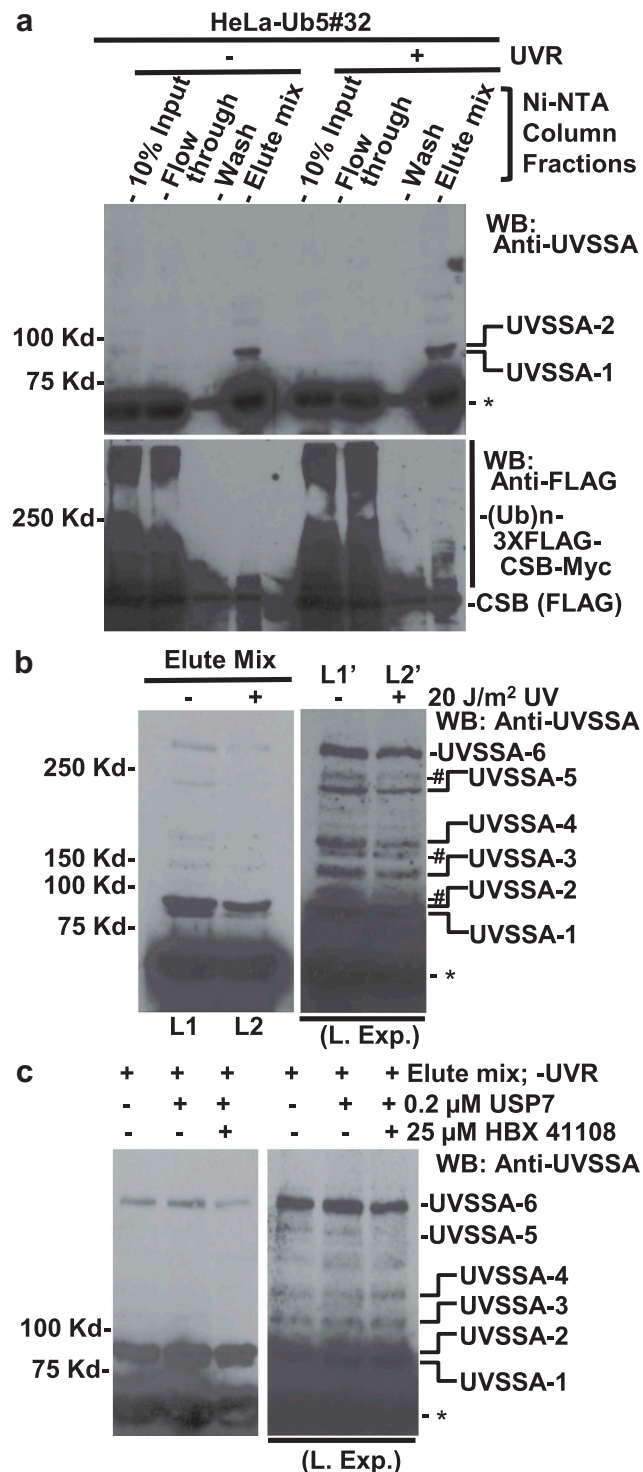


Figure 8. USP7 does not deubiquitinate Ub conjugates of UVSSA *in vitro*. (a) Ni-NTA spin column purification was used to enrich UVSSA-2 form. Cell extracts from HeLa-Ub5#32 cells were subjected to a 6xHistidine-tagged protein purification and the indicated fractions were Western blotting analyzed for modified species of UVSSA and CSB. (b) Detection of multiple UVSSA forms in concentrated eluate fractions. The eluate mixtures in Figure 8(a) were desalted and further concentrated with Amicon ultra-centrifugal filters and detected for modified forms of UVSSA. The major Ub conjugate bands were annotated as UVSSA-2 to UVSSA-6. Symbol (#) marks the minor but distinctly visible UVSSA conjugates. Asterisk (*) marks nonspecific bands in anti-UVSSA blots. (c) The USP7 deubiquitination assay was performed with Ni-NTA spin column purified Ub conjugates as described in Figure 8 (a, b). The reaction mixtures were Western Blotting analyzed for UVSSA. In reactions containing HBX 41108, the inhibitor was pre-mixed with USP7 enzyme for 30 min and followed by adding purified Ub conjugates.

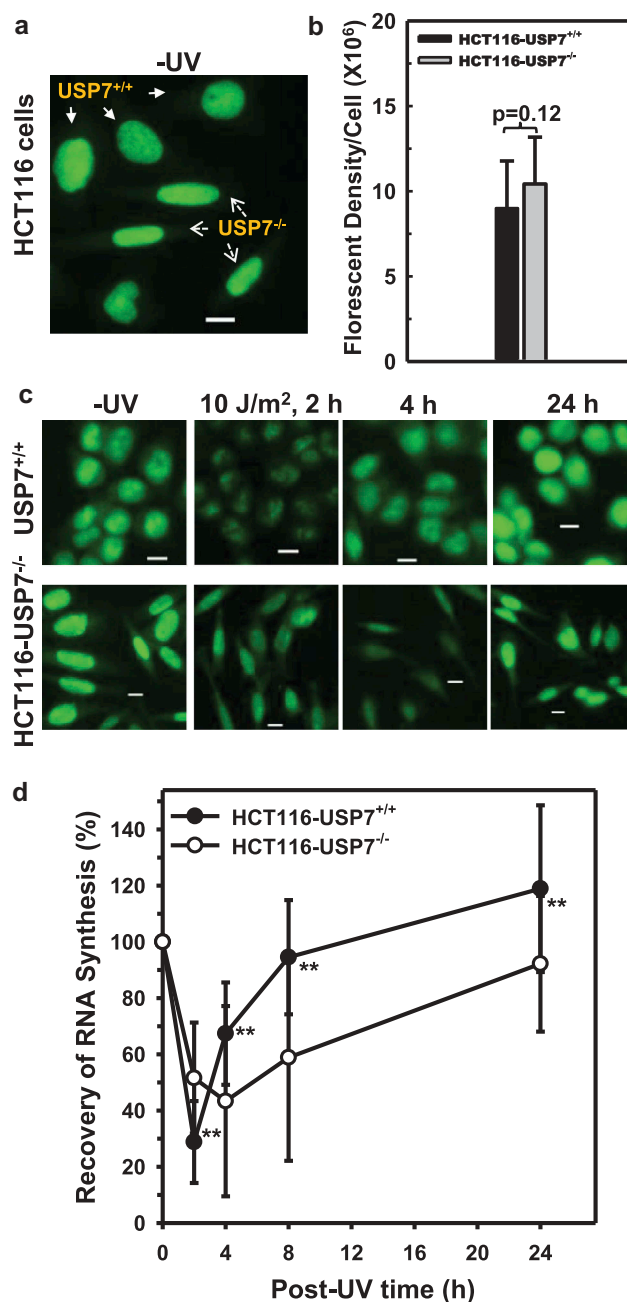


Figure 9. USP7 deficiency affects the recovery of RNA synthesis following UV irradiation. (a) The Click-iT RNA Imaging Assay was performed to detect temporal and global *de novo* RNA synthesis in HCT116-USP7^{+/+} and USP7^{-/-} cells. Different arrow types point to individual HCT116-USP7^{+/+} or USP7^{-/-} cells distinguishable by the shape of the cells and nuclei. The calibration bar is set at 10 μ m. (b) The integrated fluorescence density per cell of HCT116-USP7^{+/+} or USP7^{-/-} cells without UV irradiation. The fluorescence density was quantitated by ImageJ software. Mean \pm SD was calculated from the data of ≥ 30 independent cells across multiple microscopic fields. The p annotation indicates that p is 0.12 in Student's t-Test. (c) The Click-iT RNA Imaging Assay was performed with HCT116-USP7^{+/+} or USP7^{-/-} cells at different time points following UVR exposure. Calibration bar is 10 μ m. (d) The Click-iT RNA Imaging experiments were independently repeated ≥ 3 times. The recovery of RNA synthesis (RSS) was calculated by normalizing integrated density per cell of UVR-exposed cells against that of controls without exposure. Mean \pm SD at different time points was calculated from the data of ~ 30 -50 cells from multiple microscopic fields and from different experiments. Double-asterisk ** designates p \leq 0.01 in Student's t-test of USP7^{+/+} vs USP7^{-/-} cells at indicated time points.

We further examined the association of CSB with USP7 and UVSSA in chromatin fractions. As shown in Figure 6(b), without UVR, USP7 showed a strong presence in anti-FLAG-CSB immunoprecipitates of

soluble chromatin fraction from HeLa#57 cells. Whereas, only some shorter USP7 form was seen in immunoprecipitates with soluble chromatin fraction of HeLa-Ub5#32 cells (Figure 6(b), L1 vs. 5). UV

irradiation reduced USP7 presence in soluble chromatin fractions from both cells (Figure 6(b), L2 and 6). With insoluble chromatin, weaker USP7 signals were seen in CSB immunoprecipitates under UVR in HeLa#57 cells and regardless of UVR in HeLa-Ub5#32 cells (Figure 6(b), L4, L7, and L8). On the other hand, UVSSA presence was only seen in anti-FLAG-CSB immunoprecipitates of the soluble chromatin fraction from HeLa#57 cells. Thus, while CSB, UVSSA, and their modified forms differentially distribute in soluble and insoluble chromatin fractions, the CSB-USP7 and CSB-UVSSA associations can be demonstrated in soluble chromatin fractions.

The decreased CSB-USP7 association observed in the presence of abundant cellular CSB in soluble chromatin from HeLa-Ub5#32 could be because (i) CSB-USP7 interaction requires UVSSA, which was depleted from this fraction or (ii) the complexes containing CSB and USP7 were depleted from the soluble fraction and relocated to insoluble chromatin fraction. As both CSB and UVSSA bind with the same USP7 TRAF domain [34] (Figure 4(b)), the latter may be more likely.

The expression of FLAG- and Myc-tagged CSB in HeLa-Ub5#32 cells harboring 6xHistidine-tagged Ub enables verification of observed Ub-modified CSB forms in chromatin fractions. Under native conditions, Ni-NTA agarose enriched both the <250 and >250 Kd forms of modified CSB from HeLa-Ub5#32 cells (Figure 7(a), lanes 5–8). These forms were present in greater abundance within insoluble chromatin fractions. The >250 Kd CSB-Ub conjugates were further increased upon UV irradiation. Whereas under denaturing conditions in presence of 7 M urea, only <250 Kd CSB forms were detected in UV-irradiated cells as compared with non-UV control (Figure 7(a), lanes 9 vs 10), and this may be due to technical limitations. However, the anti-FLAG gel enriched modified CSB forms alike as Ni-NTA agarose, where the presence of both <250 Kd and >250 Kd CSB forms was confirmed.

UVSSA and its Ub conjugates were also identified in HeLa-Ub5#32 cells using Ni-NTA agarose-based enrichment of 6xHistidine-tagged Ub conjugates (Figure 7(b)). UVSSA protein band, with calculated molecular weight of 81 Kd, was observed in soluble chromatin fractions (Figure 7(b), L1 and 2). In

contrast, multiple UVSSA bands appeared in insoluble chromatin fractions regardless of cellular UV irradiation (Figure 7(b), L3 and 4). Upon enrichment by Ni-NTA agarose, multiple bands of UVSSA, larger than its calculated molecular weight, were seen in soluble chromatin fractions. These larger UVSSA species showed up at much higher intensity in insoluble chromatin fractions (Figure 7(b), L5–8). The results suggested that ubiquitinated UVSSA forms are largely associated with insoluble chromatin in human cells.

Characterization of mono- and poly-ubiquitinated UVSSA

To further validate UVSSA-Ub conjugates, we carried out the purification of Ub conjugates using Ni-NTA spin column under native conditions. As the modified UVSSA species appeared primarily in insoluble chromatin, we used the Lysis Buffer NPI-10-Ig, which contains Benzonase and 300 mM NaCl for stripping tightly chromatin-associated modified UVSSA. As shown in Figure 8(a), the UVSSA and its modified species were mostly undetectable in ~10% Input samples, whereas dual UVSSA bands were clearly present in Elute mix with both untreated and UVR-treated cells. The upper UVSSA-2 band showed greater enrichment. Judging from the molecular sizes, UVSSA-1 represents the native UVSSA with a theoretical molecular weight of 81 Kd, while UVSSA-2 would be the mono-ubiquitinated UVSSA. Aside from UVSSA, <250 Kd CSB-Ub conjugates with visible bands were seen in elute mix from the UVR-treated cells, while >250 Kd CSB-Ub conjugates were detected in flow through but not in elute mix.

As UVSSA-2 was the dominant form within soluble chromatin fractions of HeLa#57 cells (Figure 6(a), L1 and L2), and this specific form exhibited a decrease from insoluble chromatin fractions of both HeLa#57 and HeLa-Ub5#32 cells, we examined the possibility that UVSSA undergoes polyubiquitination. We concentrated the elute mix for analyzing the lesser abundant forms. UVSSA-1 and UVSSA-2 forms were distinctly visible in concentrated elute mix, and their intensities showed a mild reduction upon UV irradiation (Figure 8(b), left panel). Under

longer exposure (Figure 8(b), right panel), additional bands, i.e., UVSSA-3 to UVSSA-6 were resolved as major modified forms along with other less visible forms. As lysine 414 of UVSSA has been identified as the sole target of ubiquitination [34,35], we concluded that the chromatin-associated UVSSA exists in native, mono-ubiquitinated form and, to a lesser extent, in polyubiquitinated forms.

We also conducted an *in vitro* UVSSA deubiquitination assay using purified Ub conjugates. We did not observe any detectable decrease in poly-ubiquitinated forms of UVSSA in the presence of high concentration (0.2 μ M) of USP7 (Figure 8(c)). Thus, USP7 is not a specific DUB for UVSSA-Ub conjugates *in vitro*.

USP7 disruption does not affect RNA synthesis but reduces RRS following UVR-induced DNA damage

We compared RNA synthesis and recovery of RNA synthesis (RRS) as a function of cellular USP7 status. Comparison of RNA synthesis by Click-iT RNA imaging assay showed that USP7 disruption did not affect the integrated fluorescent density of newly synthesized RNA (Figure 9(a,b)). In contrast, UVR decreased the RNA synthesis within 2 h after UV irradiation. Meanwhile, the USP7 disruption decreased the level of RRS at 4 to 24 h of UV irradiation. Thus, the USP7 function is required for full RRS following UVR-induced DNA damage.

Discussion

USP7 has been described as a UVSSA interacting partner, which is involved in maintaining CSB level [19–21]. To gain mechanistic insights into the USP7-mediated regulation, we investigated the underlying basis of the biphasic response observed with CSB as well as UVSSA. We showed that in human cells, USP7 is required for the recovery of CSB protein but not UVSSA. We also described that USP7 interacts with CSB and VCP/p97 *via* its substrate-interacting TRAF domain, and demonstrated USP7-mediated CSB deubiquitination. We outlined the cellular distribution of CSB-Ub conjugates, showing their association with chromatin. We further described the impact of CSB

overexpression on UVSSA, UVSSA-Ub conjugates and their presence in insoluble chromatin. Additionally, we characterized the discrete mono-ubiquitinated and poly-ubiquitinated forms of UVSSA and revealed that ubiquitinated UVSSA was not cleavable *in vitro* by USP7. Lastly, our RRS imaging experiments indicated that USP7 disruption did not affect overall RNA synthesis but decreased its recovery following UVR-induced DNA damage. These interwoven molecular events depict a distinct role of USP7 in fine-tuning of TC-NER by deubiquitinating chromatin-associated CSB-Ub conjugates and disengaging them from proteolysis.

Our data show that USP7 interacts with CSB through its TRAF domain (Figure 4(b)). This is consistent with the observed deubiquitinating activity of USP7 for CSB and with the existence of TRAF recognition motif in CSB. It is peculiar that the USP7 TRAF domain also interacts with UVSSA [34] and that both UVSSA and USP7 are required for maintaining cellular CSB levels after UV irradiation (19–21). Given that UVSSA non-competitively inhibits USP7 deubiquitinating activity toward artificial substrate [34], it is unlikely that the binding of UVSSA to USP7 substrate-interacting TRAF domain enhances USP7 deubiquitinating activity toward CSB. Recently, UVSSA was found to interact with CSB through VHS domain located in the N-terminal of UVSSA [21,36]. A UVSSA mutant, which cannot be ubiquitinated and unable to bind USP7, was shown to act in restoring survival and RRS of UVSSA-deficient cells [34]. Such a UVSSA mutant can still stabilize CSB after UV irradiation in Kps3 cells [34]. These observations suggest that UVSSA can regulate CSB in both USP7-dependent and independent ways.

VCP/p97 has been shown to act in extracting ubiquitinated NER damage sensors, XPC, DDB2, CSB, and RNAPII, from chromatin and present them to proteasome for degradation [18,25,37,38]. Among these sensors, XPC, just like CSB, is a specific substrate of USP7 [25]. Thus, USP7 can deubiquitinate different substrates to prevent their proteolysis in NER. Our results showed that USP7 TRAF and UBL1 domains interact with VCP/p97 and the results are consistent with the USP7-VCP/p97 interaction revealed by mass spectrometry-based proteomic approaches [39]. Given the regulatory role of UBL domains in

USP7 activity [40–42], it is possible that VCP/p97 can modulate USP7 deubiquitinating activity toward a VCP/p97 client, e.g. CSB. Alternatively, the USP7-VCP/p97 interaction may also prevent an effective presentation of CSB-Ub conjugates to proteasome, allowing CSB to be rescued before proteolysis. These possibilities need further exploration.

In summary, the present study established USP7 as a DUB specific for CSB. The work also helped characterize the mono- and poly-ubiquitination of UVSSA. Moreover, the work suggests a key link between USP7 and VCP/p97 functions, which may allow USP7 to deubiquitinate and rescue a VCP/p97 client before its proteolysis. More in-depth future studies to gain informative insights on how CSB, UVSSA, and USP7, as well as VCP/p97, interact with each other and function in TC-NER, and how UVSSA ubiquitination is regulated during TC-NER would further clarify the mechanistic nature of these complex interactions in DNA damage processing.

Material and methods

Chemicals, DNA constructs, antibodies, and cell lines

VCP/p97 inhibitor, N², N⁴-Dibenzylquinazoline-2,4-diamine (DBeQ), was obtained from Sigma-Aldrich (St. Louis, MO 63103). Proteasome inhibitor MG132 was purchased from EMB Millipore (Billerica, MA 01821). USP7 constructs were acquired from Dr. Yanhui Xu in the Department of Biochemistry, Fudan University Medical School. The CSB-expressing constructs were generated by sub-cloning CSB cDNA into p3xFLAG-Myc-CMV expression vector from Sigma-Aldrich (St. Louis, MO 63103).

Anti-CSB (E-18 and B10) antibodies and UVSSA/KIAA1530 antibody (P-12) were purchased from Santa Cruz Biotechnology (Santa Cruz, CA 95060), while Anti-CSB antibody A301-345A and UVSSA antibody N1N2 were from Bethyl laboratories (Montgomery, TX 77356), and GeneTex (Irvine, CA 92606). Anti-FLAG M2 agarose gels, anti-FLAG M2 antibody, anti-Myc agarose affinity gels, and anti-Myc

antibody were all obtained from Sigma-Aldrich. Whereas, anti-VCP/p97, anti-USP7, histone H3, and anti-SUMO-2/3 (18H8) antibodies were products of Abcam (<http://www.abcam.com/>), Bethyl laboratories and Cell Signaling (Danvers, MA 01923), respectively. Recombinant His-USP7 enzyme was obtained from Boston Biochem (Cambridge, MA 02139).

Cell lines, cell culture, and transfection

HCT116 and HCT116-USP7^{-/-} cells, obtained from Bert Vogelstein's laboratory [24], were grown in McCoy's 5A medium supplemented with 10% FCS and antibiotics at 37°C in a humidified atmosphere of 5% CO₂. HeLa and its derivative (HeLa-Ub5), which expresses the 6xHistidine-tagged Ub [43], were grown in standard DMEM medium. The HeLa-Ub5 cell cultures were additionally supplemented with biotin (0.5 μM, Sigma Aldrich) and puromycin (1.5 μg/ml, Life technologies), when needed. The HeLa-derived stable cell lines, expressing epitope-tagged CSB, were established by transfection of p3xFLAG-Myc-CMV-CSB expression constructs into HeLa or HeLa-Ub5 cells. After the selection of G418 at 0.5 μg/ml, the transfected cells were sub-cloned and characterized for transgene expression. For transient transfection, exponentially growing cells were plated at a desired density. Plasmid DNAs were transfected into HeLa or HCT116 cell lines using Lipofectamine 2000 reagents according to protocols provided by the manufacturer (Life Technologies, Grand Island, NY 14072).

Glutathione S-transferase (GST) pull-down assay

The GST, GST-S5a and GST-USP7 fusion proteins were expressed in *E. coli* BL21 strain. The bacterial extracts were made in lysis buffer (50 mM Tris-HCl [pH 8.0], 150 mM NaCl, 1 mM EDTA, 1 mM DTT, 1% Triton X-100). In the case of GST-USP7 fusion proteins, which form an inclusion body in *E. coli*, the bacterial extracts were made in lysis buffer containing 1% Sarkosyl, followed by centrifugation to remove unresolvable debris. For GST pull-down assay, equal amount of GST fusion proteins was

immobilized on glutathione Sepharose 4B beads in binding buffer (50 mM Tris-HCl [pH 8.0], 150 mM NaCl, 0.1% (v/v) Triton X-100). The GST and GST fusion protein-loaded beads were incubated with whole-cell extracts (WCE), containing ~1.0 mg proteins, or the indicated amount of proteins, made in RIPA buffer (50 mM Tris-HCl [pH 8.0], 150 mM NaCl, 1% NP40, 0.5% deoxycholate and protease inhibitors). After incubation at 4°C for 16 h, the beads were washed 4 times with RIPA buffer and boiled in SDS sample buffer. The bound proteins were analyzed by Western blotting for the presence of XPC, USP7, CSB, XPD, XPB or VCP/p97 protein.

Cellular fractionation and immunoprecipitation

Protein fractionation and immunoprecipitation were conducted as previously described [18,38]. In particular, Benzonase nuclease was used to digest chromatin to obtain nuclease-releasable /soluble chromatin fractions. These soluble fractions were directly used for immunoprecipitation in RIPA buffer. Whereas, the insoluble chromatin fractions were dissolved by boiling in 2% SDS lysis buffer. For immunoprecipitation, insoluble chromatin fractions were diluted 20 times in RIPA buffer, centrifuged at 15,000xg for 15 min and then the supernatants used. The immunoprecipitations were done with appropriate antibodies in RIPA buffer at 4°C overnight. The immunocomplexes were captured by protein A Plus G agarose beads. Whereas, the anti-FLAG, or anti-Myc affinity gels or Ni-NTA agarose were directly used to capture tagged proteins.

Purification of histidine-tagged Ub conjugates

Protein purifications with Ni-NTA spin column were carried out under both native and denaturing conditions, according to protocols described by provider QIAGEN (Germantown, MD 20,874). Briefly, HeLa Ub5#32 cells were rinsed twice with cold PBS and suspended in Lysis Buffer (NPI-10-Ig) with freshly added Benzonase nuclease. After 30 min incubation on ice, the lysates were centrifuged at 12,000xg for 30 min at 4 °C to collect the supernatant. The

cleared supernatant was loaded onto the pre-equilibrated Ni-NTA spin column (twice, ~600 µl each). The loaded Ni-NTA spin columns were washed twice with Buffer NPI-20 and then eluted twice with Buffer NPI-500. The pooled elute mix was used immediately for Western blotting analysis or kept at -80°C, after adding 25% Glycerol. For *in vitro* deubiquitination assay, the stored elute mix was further processed with Amicon Ultra Centrifugal Filter Devices to remove salts, imidazole and to exchange to DUB buffer. The purifications under denaturing conditions were done according to QIAGEN protocol, where Lysis Buffer containing 7 M urea was used for dissolving HeLa Ub5#32 cells or insoluble chromatin fractions.

In vitro CSB and UVSSA deubiquitination assay

For CSB deubiquitination assay, the anti-FLAG affinity agarose beads were loaded with FLAG-tagged CSB and its modified species by incubating the beads with the soluble chromatin or 20-fold diluted insoluble chromatin fractions in RIPA buffer at 4°C overnight. The beads were washed 3 times with RIPA buffer and twice with DUB buffer (50 mM Tris-Cl [pH 8.0], 50 mM NaCl, 1 mM EDTA, 5% glycerol, 10 mM DTT), followed by 2 h incubation at room temperature with 0.2 µM USP7 in 50 µl of DUB buffer. After the reaction, the anti-FLAG beads were washed twice with DUB buffer and boiling in SDS sample buffer and Western blotting analyzed for FLAG-tagged CSB.

The UVSSA deubiquitination assays were carried out with Ub conjugates purified by Ni-NTA spin column under native conditions. A 50 µl-reaction contained 25 µl of desalted elute mix in DUB buffer and the reaction was initiated by mixing the substrates with USP7 at a final concentration of 0.2 µM and incubating at room temperature for 2 h. When HBX 41,108 was used, the recombinant USP7 was first incubated with HBX 41,108 at room temperature for 30 min before adding substrates. The deubiquitination reactions were stopped by boiling in SDS sample buffer and analyzed by Western blotting for UVSSA.

Nascent RNA imaging

HCT116 and HCT116-USP7^{-/-} cells were seeded onto glass coverslips and grown for 24 to 48 h. The coverslips were subjected to UV irradiation at 10 J/m². The UVR-treated or untreated cells were allowed to DNA repair for indicated periods and were then labeled with 1 mM 5-ethynyl uridine (EU) for 1 h, rinsed with cold PBS and then fixed with 2% paraformaldehyde. The incorporated EU was revealed with Click-iT RNA imaging kit (Invitrogen) according to the manufacturer's instruction. The images were captured using Nikon fluorescence microscope equipped with NIS software.

Quantitative analysis and statistics

Quantitative analysis was done on digitalized Western blotting images using ImageJ software and the relative protein amounts were calculated based on gray density. The ImageJ software was also used for measuring pixel and intergraded density of the interested area of Click-iT RNA fluorescent images. The Student's *t*-tests for paired comparison were performed on the data from experiments repeated ≥ 3 times, using SigmaPlot software.

Acknowledgments

Authors thank Dr. Bert Vogelstein for providing HCT116, HCT116-p53^{-/-} and HCT116-USP7^{-/-} cell lines. Authors are also grateful to Drs. Yanhui Xu at Department of Biochemistry, Fudan University Medical School and Dr. Yang Shi at Department of Cell Biology, Harvard Medical School for providing expression constructs of USP7. This work was supported by Public Health service Grants (ES2388, ES12991) from the National Institute of Health.

Disclosure statement

No potential conflict of interest was reported by the authors.

Funding

This work was supported by the National Institute of Environmental Health Sciences [ES012991].

References

- [1] Ljungman M. The DNA damage response – repair or despair? *Environ Mol Mutagen*. 2010;51:879–889.
- [2] Nospikel T. DNA repair in mammalian cells: nucleotide excision repair: variations on versatility. *Cell Mol Life Sci*. 2009;66:994–1009.
- [3] Sugawara K. Regulation of damage recognition in mammalian global genomic nucleotide excision repair. *Mut Res*. 2010;685:29–37.
- [4] De Laat WL, Jaspers NG, Hoeijmakers JH. Molecular mechanism of nucleotide excision repair. *Genes Dev*. 1999;13:768–785.
- [5] Ford JM, Hanawalt PC. Role of DNA excision repair gene defects in the etiology of cancer. *Curr Top Microbiol Immunol*. 1997;221:47–70.
- [6] Petit C, Sancar A. Nucleotide excision repair: from *E. coli* to man. *Biochimie*. 1999;81:15–25.
- [7] Hanawalt PC, Spivak G. Transcription-coupled DNA repair: two decades of progress and surprises. *Nat Rev Mol Cell Biol*. 2008;9:958–970.
- [8] Spivak G. UV-sensitive syndrome. *Mutat Res*. 2005;577:162–169.
- [9] Schwertman P, Vermeulen W, Marteijn JA. UVSSA and USP7, a new couple in transcription-coupled DNA repair. *Chromosoma*. 2013;122:275–284.
- [10] van Gool AJ, Citterio E, Rademakers S, et al. The Cockayne syndrome B protein, involved in transcription-coupled DNA repair, resides in an RNA polymerase II-containing complex. *Embo J*. 1997;16:5955–5965.
- [11] van dB V, Citterio E, Hoogstraten D, et al. DNA damage stabilizes interaction of CSB with the transcription elongation machinery. *J Cell Biol*. 2004;166:27–36.
- [12] Svejstrup JQ. Mechanisms of transcription-coupled DNA repair. *Nat Rev Mol Cell Biol*. 2002;3:21–29.
- [13] Anindya R, Aygun O, Svejstrup JQ. Damage-induced ubiquitylation of human RNA polymerase II by the ubiquitin ligase Nedd4, but not Cockayne syndrome proteins or BRCA1. *Mol Cell*. 2007;28:386–397.
- [14] Bregman DB, Halaban R, van Gool AJ, et al. UV-induced ubiquitination of RNA polymerase II: a novel modification deficient in Cockayne syndrome cells. *Proc Natl Acad Sci U S A*. 1996;93:11586–11590.
- [15] Vermeulen W, Fousteri M. Mammalian transcription-coupled excision repair. *Cold Spring Harb Perspect Biol*. 2013;5:a012625.
- [16] Fousteri M, Vermeulen W, Van Zeeland AA, et al. Cockayne syndrome A and B proteins differentially regulate recruitment of chromatin remodeling and repair factors to stalled RNA polymerase II in vivo. *Mol Cell*. 2006;23:471–482.
- [17] Groisman R, Kuraoka I, Chevallier O, et al. CSA-dependent degradation of CSB by the ubiquitin-proteasome pathway establishes a link between complementation factors of the Cockayne syndrome. *Genes Dev*. 2006;20:1429–1434.

- [18] He J, Zhu Q, Wani G, et al. Valosin-containing protein (VCP)/p97 segregase mediates proteolytic processing of cockayne syndrome Group B (CSB) in damaged chromatin. *J Biol Chem.* **2016**;291:7396–7408.
- [19] Zhang X, Horibata K, Saijo M, et al. Mutations in UVSSA cause UV-sensitive syndrome and destabilize ERCC6 in transcription-coupled DNA repair. *Nat Genet.* **2012**;44:593–597.
- [20] Schwertman P, Lagarou A, Dekkers DH, et al. UV-sensitive syndrome protein UVSSA recruits USP7 to regulate transcription-coupled repair. *Nat Genet.* **2012**;44:598–602.
- [21] Nakazawa Y, Sasaki K, Mitsutake N, et al. Mutations in UVSSA cause UV-sensitive syndrome and impair RNA polymerase II processing in transcription-coupled nucleotide-excision repair. *Nat Genet.* **2012**;44:586–592.
- [22] Meulmeester E, Maurice MM, Boutell C, et al. Loss of HAUSP-mediated deubiquitination contributes to DNA damage-induced destabilization of Hdmx and Hdm2. *Mol Cell.* **2005**;18:565–576.
- [23] Li M, Chen D, Shiloh A, et al. Deubiquitination of p53 by HAUSP is an important pathway for p53 stabilization. *Nature.* **2002**;416:648–653.
- [24] Cummins JM, Rago C, Kohli M, et al. Tumour suppression: disruption of HAUSP gene stabilizes p53. *Nature.* **2004**;428:1.
- [25] He J, Zhu Q, Wani G, et al. Ubiquitin-specific protease 7 regulates nucleotide excision repair through deubiquitinating XPC protein and preventing XPC protein from undergoing ultraviolet light-induced and VCP/p97 protein-regulated proteolysis. *J Biol Chem.* **2014**;289:27278–27289.
- [26] Zhu Q, Sharma N, He J, et al. USP7 deubiquitinase promotes ubiquitin-dependent DNA damage signaling by stabilizing RNF168. *Cell Cycle.* **2015**;14:1413–1425.
- [27] Fei J, Chen J. KIAA1530 protein is recruited by Cockayne syndrome complementation group protein A (CSA) to participate in transcription-coupled repair (TCR). *J Biol Chem.* **2012**;287:35118–35126.
- [28] Sin Y, Tanaka K, Saijo M. The C-terminal region and SUMOylation of cockayne syndrome group b protein play critical roles in transcription-coupled nucleotide excision repair. *J Biol Chem.* **2016**;291:1387–1397.
- [29] Layfield R, Tooth D, Landon M, et al. Purification of poly-ubiquitinated proteins by S5a-affinity chromatography. *Proteomics.* **2001**;1:773–777.
- [30] Higa M, Zhang X, Tanaka K, et al. Stabilization of ultraviolet (UV)-stimulated scaffold protein a by interaction with ubiquitin-specific peptidase 7 is essential for transcription-coupled nucleotide excision repair. *J Biol Chem.* **2016**;291:13771–13779.
- [31] Kim RQ, Sixma TK. Regulation of USP7: a High Incidence of E3 Complexes. *J Mol Biol.* **2017**;429:3395–3408.
- [32] Cheng J, Li Z, Gong R, et al. Molecular mechanism for the substrate recognition of USP7. *Protein Cell.* **2015**;6:849–852.
- [33] Zhu Q, Wani AA. Nucleotide excision repair: finely tuned molecular orchestra of early pre-incision events. *Photochem Photobiol.* **2017**;93:166–177.
- [34] Higa M, Tanaka K, Saijo M. Inhibition of UVSSA ubiquitination suppresses transcription-coupled nucleotide excision repair deficiency caused by dissociation from USP7. *Febs J.* **2018**;285:965–976.
- [35] Elia AE, Boardman AP, Wang DC, et al. Quantitative proteomic atlas of ubiquitination and acetylation in the DNA damage response. *Mol Cell.* **2015**;59:867–881.
- [36] Ogi T, Nakazawa Y, Sasaki K, et al. Molecular cloning and characterisation of UVSSA, the responsible gene for UV-sensitive syndrome. *Seikagaku.* **2013**;85:133–144.
- [37] Puumalainen MR, Lessel D, Ruthemann P, et al. Chromatin retention of DNA damage sensors DDB2 and XPC through loss of p97 segregase causes genotoxicity. *Nat Commun.* **2014**;5:3695.
- [38] He J, Zhu Q, Wani G, et al. UV-induced proteolysis of RNA polymerase II is mediated by VCP/p97 segregase and timely orchestration by Cockayne syndrome B protein. *Oncotarget.* **2016**;8:11004–11019.
- [39] Xue L, Blythe EE, Freiburger EC, et al. Valosin-containing protein (VCP)-Adaptor Interactions are exceptionally dynamic and subject to differential modulation by a VCP inhibitor. *Mol Cell Proteomics.* **2016**;15:2970–2986.
- [40] Faesen AC, Dirac AM, Shanmugham A, et al. Mechanism of USP7/HAUSP activation by its C-terminal ubiquitin-like domain and allosteric regulation by GMP-synthetase. *Mol Cell.* **2011**;44:147–159.
- [41] Faesen AC, Luna-Vargas MP, Sixma TK. The role of UBL domains in ubiquitin-specific proteases. *Biochem Soc Trans.* **2012**;40:539–545.
- [42] Rouge L, Bainbridge TW, Kwok M, et al. Molecular understanding of USP7 substrate recognition and C-terminal activation. *Structure.* **2016**;24:1335–1345.
- [43] Tagwerker C, Flick K, Cui M, et al. A tandem affinity tag for two-step purification under fully denaturing conditions: application in ubiquitin profiling and protein complex identification combined with in vivocross-linking. *Mol Cell Proteomics.* **2006**;5:737–748.